

Design and Implementation of High-Gain Wide-Bandwidth Patch Antenna Array 5G Base Stations

Qahtan Mutar Gatea¹, Faris Mohammed Ali¹

¹Department of Techniques Communications Engineering, Engineering Technical College, Al-Furat Al Awsat Technical University.

Corresponding Author Email: qahtan9112@gmail.com

Received Apr.17, 2025

Revised Jun.11, 2025

Accepted Jun.14, 2025

Online Sept.1, 2025

ABSTRACT

This article introduces an analysis and design of an array of elements consisting of four antenna elements connected by a power divider. This proposed antenna demonstrates superior performance for 5G base station mmWave applications. The 1 x 4 T-junction power divider feeding technique was used in the design of these arrays. This power divider provided an easy model, low spurious radiation, and the best bandwidth. This work presents an antenna array simulated with the High-Frequency Structure Simulator tool (HFSS) working at a resonant frequency of 28 GHz. The substrate material is Rogers 4003, with a layer thickness of 0.4 mm, permittivity of 3.5, and a loss tangent value of 0.0027. The results of simulations derived from this research work are as follows: VSWR 1.09, S11 -34 dB, gain 11 dB, bandwidth 2.56 GHz, directivity 11.1 dB, efficiency 96%. This proposed 5G base station array antenna has achieved enhanced performance compared to other antenna array designs. Consequently, it is positioning it as a significant contender for 5G applications.

Keywords: Microstrip Patch Antenna, Power Divider, 1x4 Antenna Array, mmWave, 5G Base Station, defected ground structure (DGS), voltage standing wave ratio VSWR.

1. Introduction

Growing requirements and utilization in different fields of wireless communication system devices, such as aeronautics, defense, and medicine, drive producers to consistently develop wireless systems. From this perspective, In recent years, microwave circuit technology has seen significant progress [1-4]. The antenna element in the communication system chain occupies a large space, which means an extra footprint that hinders its incorporation into the small spaces, especially in fifth-generation stations, which are characterized by a high distribution density of base stations, their miniaturization plays an essential role in concealing their features in the areas of their deployment. Patch and microstrip antennas are fundamental elements for the 5G base station due to numerous features such as low cost, compact size, and simple installation on electronic circuits, vehicles, airplanes, and satellites. Nonetheless, these antennas face limitations such as narrow bandwidth and low gain, restricting their use in certain scenarios [5-6]. The 5G in mmWave has high frequencies greatly impacted by antenna radiator performance, particularly gain, bandwidth, and return loss. Therefore, it is necessary to design antennas with a gain of at least 8 dB to meet the requirements of the fifth generation at high frequencies. To address these challenges and achieve subscriber requirements, it is necessary to develop antenna elements with suitable characteristics for the bandwidth, return loss, and gain [7-8]. Up to 100 Mbps of data transfer rate is possible with 5G technology, while current demand is expected to surpass 10 Gbps. Consequently, a wireless communication technique that fulfills these requirements, designated the 5G network, is essential. The latter provides 10 Gbps of data transfer rate and broad coverage of one million components on 1 km², with network access of 10.1 Tbps on 1 km², a response time not exceeding one millisecond, and among other features things [9-11]. To fulfill all the aforementioned needs and get satisfactory outcomes with 5G, it is essential to use the mmWave. In this context, certain frequency bands for 5G were delineated within the following intervals: 3.4-3.6 GHz, 5.1GHz-5.8 GHz, 24 GHz-28.5 GHz, 38 GHz-40 GHz, and 65 GHz-77 GHz, which were defined by

federal commission for communications (FCC) and international telecommunication union (ITU) [1- 2]. We selected the 28 GHz spectrum for our study because the antenna performs well in 5G and is in trial use in numerous nations. The antenna for the 5G base stations must exhibit optimal performance, including high gain, directivity, and wide bandwidth, to fulfill consumer expectations and needs involving high data rates of 5G modern technology [3][12]. Typically, the 5G base stations network typically requires low-weight, high-performance subarrays that are compact in size, simple to install, and low in cost. A patch antenna is an essential element in a base station, prompting studies to focus on this area. This article is, therefore, significantly reliant on the patch radiator. In connection with this advancement, the demands and necessities of the wireless network have escalated considerably. Wireless network standards have lately emerged to address these difficulties every decade following the establishment of the subsequent generation of standards [13- 15]. Several studies relate to designing and analyzing mmWave band patch antennae for 5G base stations, particularly in the 28 GHz band. Due to this reason, it is essential to create new patch antenna types appropriate for these networks. It is a complex undertaking and a significant obstacle for experts in antenna design. Consequently, they offered various antennas, such as the patch antenna [6], with a gain value of 12 dB. However, they do not ensure optimal impedance matching -14 dB with dimensions of 53x20 mm.

4 Quasi-Yagi antenna array elements proposed in [7] Realized 9.98 dBi gain measuring 20x8.4 mm in size. The reference [8] Also suggests constructing and designing an antenna array with eight radiators that realizes a peak gain value of 9.6 dB, but it is inappropriate for 5G technologies. In [9], the printed element structure within a metal enclosure achieves a gain exceeding 10 dB at 28 GHz. A printed antenna array design is introduced in [10] With four elements, with a gain value of 13 dB. In [11] An array antenna structure comprises eight elements, which attained a gain of 9.4 dB at 28 GHz. However, the structure is highly expensive. In [12] design and optimization of a two-band antenna with rectangular slot-pi to realize a wide bandwidth in two bands from 27.3–34.2 GHz and 34.7–38.6 GHz, respectively, had been proposed. In [13], a high-gain, frequency-switched, miniaturized antenna with stubs is discussed. These sections permit changes in frequency from 28.2 GHz to 24.6 GHz with over 15 dB gain and 2.1 GHz and 1.9 GHz bandwidth, respectively. This antenna is not compatible with 5G stations because it does not need to reconfigure the frequency. A helical antenna with a single hole for broadband 5G application at sub-6GHz is suggested in [14] with 3.89 GHz and 5.83 dB as bandwidth and gain, respectively, and 85% radiation efficiency. Patch antennas with parasitic elements have been suggested to improve gain, and a band was introduced in [15]. The authors in [16] Introduced a compact wide-bandwidth patch antenna. A Defected Ground Structure (DGS) was integrated into the ground layer of a single element in this array to significantly enhance bandwidth. In [17] the authors introduced a 28 GHz inspired-helical end-fire antenna. This antenna features a straightforward design derived from a traditional planar helix antenna without incorporating vias. It provides a gain value of 5.7 dB, an impedance bandwidth of 3.7 GHz, and a radiation array efficiency of 86%. The authors in [18] introduced a flat rectangular patch radiator, including slots in the ground plane and the patch structure. It realized a peak gain value of 8.6 dB and an impedance bandwidth value of 2.7 GHz. Certainly, the 5G base station applications system needs antenna radiators with superior performance regarding return loss, efficiency, gain, impedance bandwidth, and size. To fulfill this requirement, we suggest a novel radiator array antenna design that involves four patch radiators in a linear array with shapes like a Burning Head. There are many slots in antenna design to improve the antenna performance. The 1x4 array antenna radiators operate at 28 GHz and are suitable for use in 5G MIMO applications.

2. Methodology

This section outlines the final antenna array design in three primary stages. The initial phase starts with the design of a single antenna operating at 28 GHz. In the second stage, a T-shaped power divider is engineered to ensure uniform power distribution between the four elements while achieving a phase shift of zero degrees. At this step, the power divider's performance is tuned to enhance efficiency and minimize losses incurred during the division process. This seeks to facilitate the third phase, which entails the construction of an antenna array, including four elements that function cohesively to get the desired performance.

2.1 Microstrip Patch Antenna

According to the transmission feed line model theory used to characterize microstrip patch antennas, a direct approach design can be executed for the proposed antennas. This approach facilitates the identification of fundamental parameters, such as the desired frequency and the electrical characteristics of the substrate utilized, substrate height, and permittivity, to provide optimal antenna performance following the required specifications.

Consequently, we designate $\epsilon_r=3.5$, height=0.4 mm, and frequency=28 GHz. The initial step involves calculating the patch size based on the substrate's properties (height, permittivity) and the resonance frequency. The microstrip feed line distributes power to the radiator. We selected Roger 4003C as an essential substrate material due to its high quality and price. The selected features are 28 GHz as an operating frequency of substrate Rogers 4003 with 3.5 permittivity. This microstrip transmission line is extensively utilized in the manufacturing of microwave circuits due to it is compatible with photolithographic processes. It facilitates the straightforward incorporation of active and passive parts through surface installation [19-22].

$$E_s \leq \frac{0.3 \times c}{2\pi f_{res} \sqrt{\epsilon_r}} \quad (1)$$

$$W_{patch} = \frac{c}{2f_{res}} \sqrt{\frac{2}{\epsilon_r + 1}} \quad (2)$$

$$\epsilon_{eff} = \frac{\epsilon_r + 1}{2} + \frac{\epsilon_r - 1}{2} \left(1 + 12 \frac{E_s}{W_p}\right)^{-1} \quad (3)$$

$$L_{eff} = \frac{c}{2 \times f_{res}} \epsilon_{eff} - \frac{1}{2} \quad (4)$$

$$\Delta L = 0.412 \frac{(\epsilon_{eff} + 0.3) \left(\frac{W_{patch}}{H_s} + 0.264\right)}{(\epsilon_{eff} - 0.258) \left(\frac{W_p}{E_s} + 0.8\right)} \quad (5)$$

$$L_p = L_{eff} - 2\Delta L_p = \frac{c}{2 \times f \times \sqrt{\epsilon_{eff}}} - 2\Delta L_p \quad (6)$$

$$W_g = W_p + 6E_s \quad \text{and} \quad L_g = L_p + 6E_s \quad (7)$$

$$W_{fed} = \frac{2h}{\pi} \left[B - 1 - \ln(2B - 1) + \frac{\epsilon_r - 1}{2\epsilon_r} \left(\ln(B - 1) + 0.39 - \frac{0.61}{\epsilon_r} \right) \right] \quad (8)$$

$$B = \frac{z_c}{60} \left(\frac{\epsilon_r + 1}{2} \right)^{0.5} + \frac{\epsilon_r - 1}{\epsilon_r + 1} \left(0.23 + \frac{0.11}{\epsilon_r} \right) \quad (9)$$

$$L_{fed} = 3E_s \quad \text{and} \quad Z_c = 50\Omega \quad (10)$$

$$|S_{11}|^2 = \frac{|z_e - z_c|^2}{|z_e + z_c|^2} \quad (11)$$

E_s denotes the diameter of the roger substrate upon which an radiator is inscribed C is light speed, f_{res} is the resonant frequency, W_p patch width, L_p patch length, ϵ_{eff} is the effective dielectric constant, ΔL_p is length extension of plate, L_g ground plant length, W_g ground plate width, W_{fed} feed line width, L_{fed} feed line length, and S_{11} is the coefficient of reflection.

The proposed patch antenna shown in Figure 1 was designed using the theoretical equations described previously. All the main and sub-dimensions of the antenna were precisely determined to ensure the required performance was achieved within the desired frequency range. These dimensions include the patch's width and length, the insulating layer's thickness, and the material's dielectric constant. All the numerical values of these dimensions are detailed in Table 1 to facilitate the repetition and testing processes in similar applications. In addition to carefully selecting the previous antenna parameters, the final antenna shape, based on placing a number of slots in the design, came to increase the antenna's matching well.

2.2 Design 1x4 Power divider

A power divider network is a linear, passive electrical component based on Ohm's law, making it an essential device in microwave and RF systems. Its principal role is enabling the combination or division of signal power, ensuring effective signal distribution. Power dividers are often designed to deliver in-phase output signals and are uniformly distributed throughout the output ports. A 1x2 T-junction power divider typically achieves an output power division ratio of 3 dB, while a 1x4 has 6 dB. These attributes render power dividers essential in applications such as antenna array feeding, signal processing, and multi-channel communication systems.

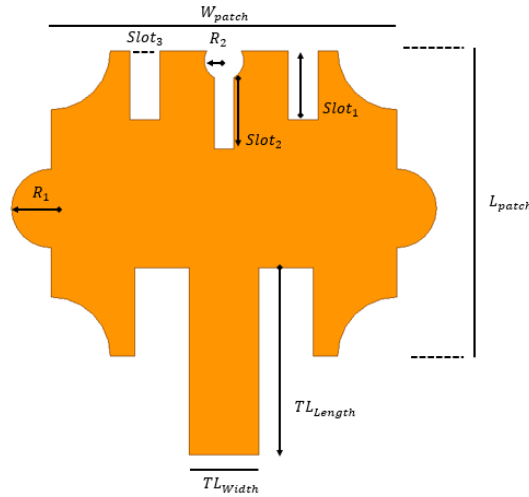


Figure 1. The Proposed Antenna Shapes.

Table1.The Proposed Single Antenna Characteristic.

Parameter	Values
W_{Patch}	3.5 mm
L_{Patch}	3.1mm
$Slot_1$	0.7mm
$Slot_2$	1mm
$Slot_3$	0.3mm
TL_{length}	1.9mm
R_1	0.4mm
R_2	0.2mm

The power divider's design is primarily depending on the microstrip lines, which are a widely used approach in circuit executions due to their ease of fabrication and compactness. The microstrip line widths corresponding to Z_{50} , Z_{100} , and Z_{70} are carefully established with conventional analytical equations, guaranteeing excellent impedance matching and low signal reflection. These computations are essential for attaining the required power distribution and preserving the integrity of the output signals. The equations that relate between microstrip line widths and their respective impedances are outlined in equation 12, in addition to equations (8) and (9). These equations establish the foundation for the accurate geometric arrangement of the power divider [23] [24] [25].

$$Z = \frac{120\pi}{\sqrt{\epsilon_r} \left(\frac{W_{50}}{h} + 1.393 + 0.0667 \ln \left(\frac{W_{50}}{h} + 1.44 \right) \right)} = < \frac{126}{\sqrt{\epsilon_r}} \quad (12)$$

Figure 2 illustrates the intricate design of the T-junction (1×4), emphasizing the geometric arrangement and the meticulously allocated lines to get the necessary power division and guarantee wave compatibility between the inputs and outputs. The simulation utilized HFSS (High-Frequency Structure Simulator), a sophisticated instrument for analyzing the electromagnetic characteristics of high-frequency models. The integration of theoretical analysis and accurate simulation with HFSS guarantees a design that fulfills the system's technical specifications. Figure 3 shows the simulation results of a 1 x 4 T junction power divider S parameters. Figure 3(a) illustrates the magnitudes of the reflection coefficients S11, S12, S13, S14, and S15 in decibels as a function of frequency. The structure exhibits a broad bandwidth of 12 GHz (ranging from 15 to 36 GHz), demonstrates minimal loss at the operational frequency of 32 GHz with S11 = -36 dB, and presents transmission coefficient with values of S12 = -6.45 dB, S13 = -7.79 dB, S14 = -7.73 dB, and S15 = -6.25 dB, which are nearly uniform and approximate the ideal value of 6 dB. Consequently, the input power was partitioned into six equal portions. Figure 3. (b) illustrates the phase values of S15, S14, S12, and S12 as a function of frequency. This figure indicates that these parameter results are in significant

agreement. At the wanted band, the phase values of parameters S15, S14, S13, and S12 are -2.6° , 7.9° , 7.6° , and -2.43° , respectively.

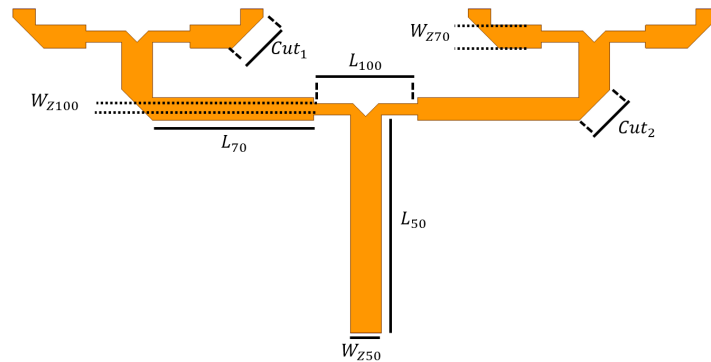


Figure 2. The junction power divider, $L_{50}=7.05\text{mm}$, $L_{100}=3.2\text{mm}$, $Cut_1=1\text{mm}$ and $Cut_2=0.95\text{mm}$.

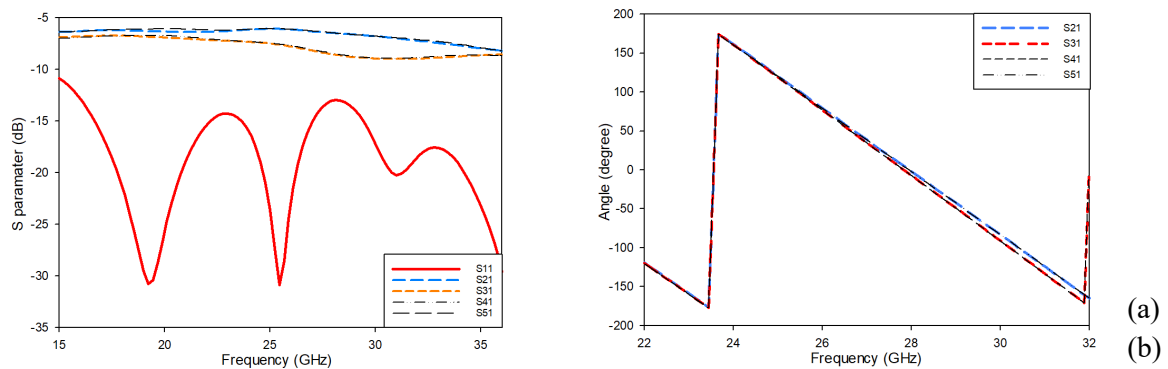


Figure 3. junction Power divider (a) Reflection coefficient (b) Phases.

2.3 Microstrip Patch Antenna Array

This study involves the structure configuration of linear array consisting of four antenna radiators, which are interconnected via a power divider to enhance the antenna system's performance significantly. This design seeks to augment gain and boost directivity properties, hence improving radiation efficiency and focus in the intended direction. This constitutes the third segment of the study since it amalgamates prior endeavors to create a cohesive antenna system that facilitates high-performance wireless communication applications. The 1×4 linear array design is shown in Figure 4.

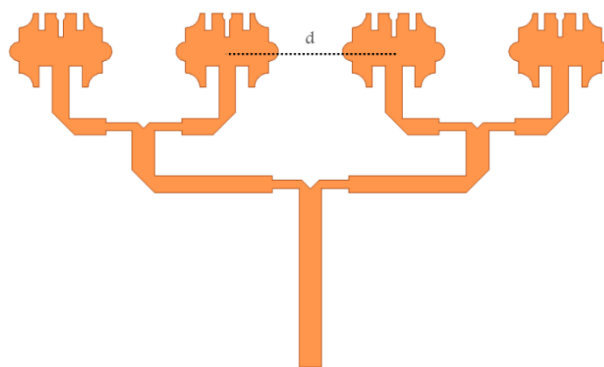


Figure 4. 1×4 Linear flame shape antenna array with $d=\lambda/2$ space between array elements.

3. Final Simulation Results and Discussion

A radiator is connected to the signal source via a feed line with a characteristic impedance of Z_c . Impedance matching is crucial for optimal power transmission between the antenna and the feeder. The compatibility eliminates the reflection power at the input of the radiator. The VSWR defines radiator matching. A VSWR of 1 indicates perfect matching, with acceptable matching present for $1 \leq \text{SWR} < 2$. While the minimum value is a perfect compatibility, matching is present for $1 \leq \text{SWR} < 2$. Optimal power transmission occurs when the antenna's input impedance matches that of the generator. Following the antenna design informed by the transmission model conclusions, we will review the proposed radiator simulation outcome in the HFSS tools. Figure 5 presents a single-patch antenna's reflection coefficient S11 curve with a value of -27.37 dB for an operating frequency of 28 GHz. Furthermore, the bandwidth is 1.1 GHz (27.4-28.5 GHz). Figure 6 illustrates a three-dimensional gain, while the VSWR of the proposed antenna is shown in Figure 7, and while current distribution is shown in Figure 8. Using a single-piece radiator often fails to meet established radiation requirements. Specific characteristics, such as an HPBW and gain, are often attainable only by aggregating many radiating sources into a configuration known as an antenna array [26][27]. The construction of many main antennas facilitates the generation of highly directional radiation, contingent upon the quantity and characteristics of the radiators, the configuration of their power source, and the technical layout of the array. The optimal feed line selection depends on various factors, including desired antenna gain, bandwidth, beam angle, insertion loss, radiation sidelobe levels, array polarization, and feed management capabilities. We chose the T-junction Power divider type as a feed line due to its ultra-wideband and lower insertion loss. Increasing the number of antennas in an antenna array generally enhances its performance. We presented a linear array of four antenna components in Figure 4 to create an antenna with better efficiency and attain the required results of the study.

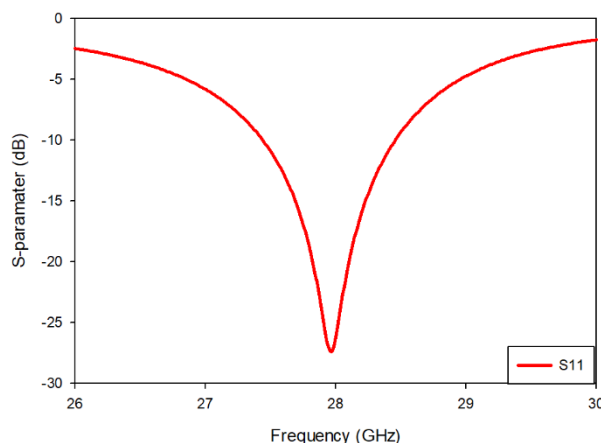


Figure 5. Reflection coefficient of a single antenna element.

The linear array's performance results were presented after conducting simulations. Figure 9 shows the extended frequency range of the variety between 26.2 and 28.76 GHz, with the best matching of the reflection coefficient at -34 dB, reflecting high efficiency in reducing the loss resulting from reflection. The final array gain was represented by two different patterns: the 3D pattern and the normalized gain pattern, as shown in Figures 10 and 11, respectively. These figures show the array's radiation performance from two different perspectives that reflect the design's compatibility with the specified objectives. Figures 12, respectively, show the 2D radiation pattern. This figure illustrates the array's improved directivity characteristics, which enhance its effectiveness in directing the radiated energy toward the desired direction. Figure 13 shows the fabricated antenna array placed on the measuring device, while Figures 14 and 15 show the measured S11 value practically after the manufacturing process and antenna array radiation efficiency, respectively.

Table 2 presents performance metrics comparing the proposed new antenna at 28 GHz with existing models. These involve VSWR, S11, bandwidth, efficiency, and gain. The study [28] exhibits a greater bandwidth than the previous studies' results, as seen in Table 2. However, it also involves more antenna components than those detailed in [39]-[44]. Conversely, it also possesses a drawback: the quantity of antenna components exceeds that of the works delineated in Table 2.

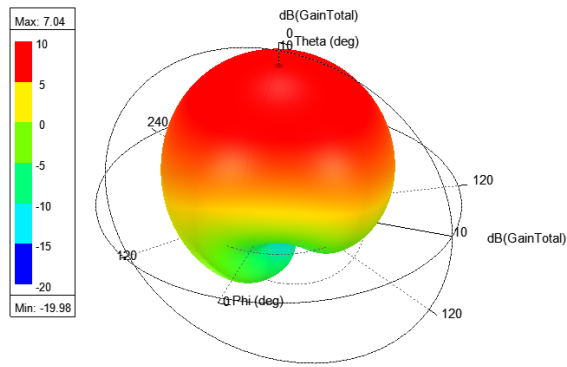


Figure 6: 3D single antenna gains

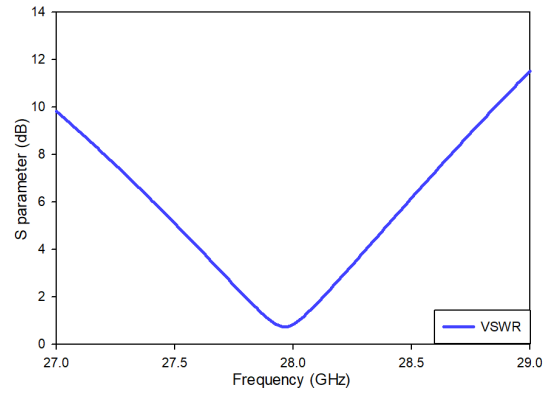


Figure 7: Single antenna VSWR

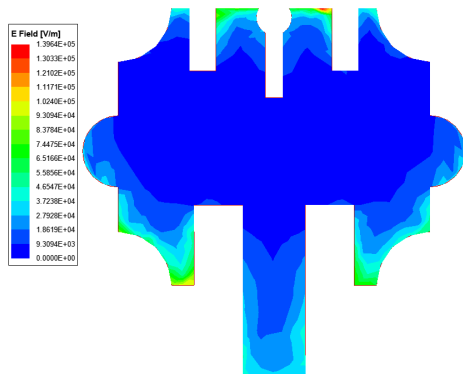


Figure 8: Single antenna current distribution.

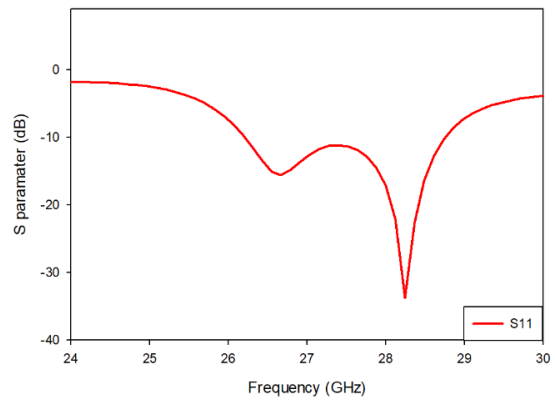


Figure 9: Reflection coefficient of array.

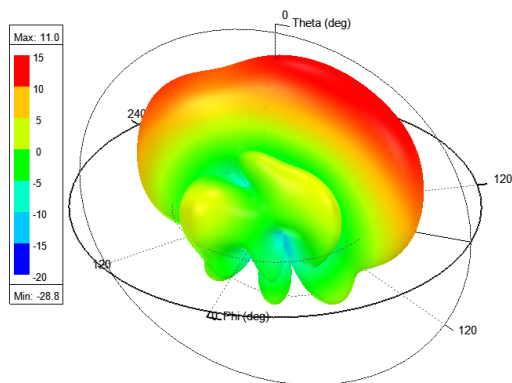


Figure 10. 3D array antenna gain.

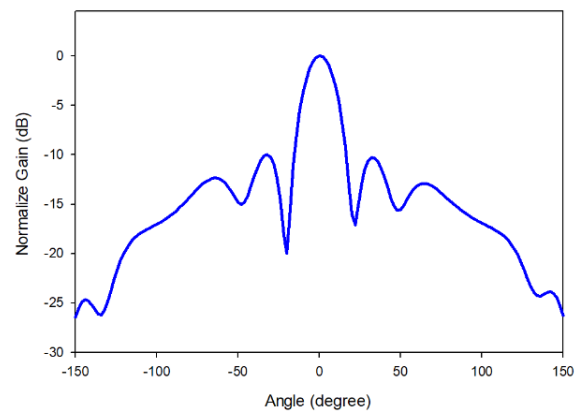


Figure 11. Normalized gain Vs Theta.

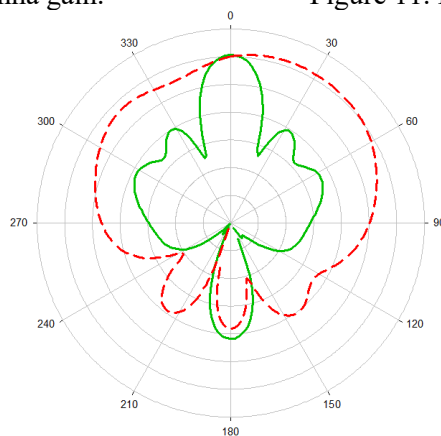
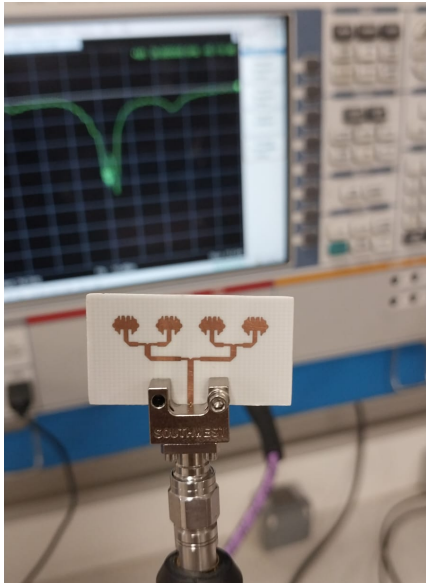
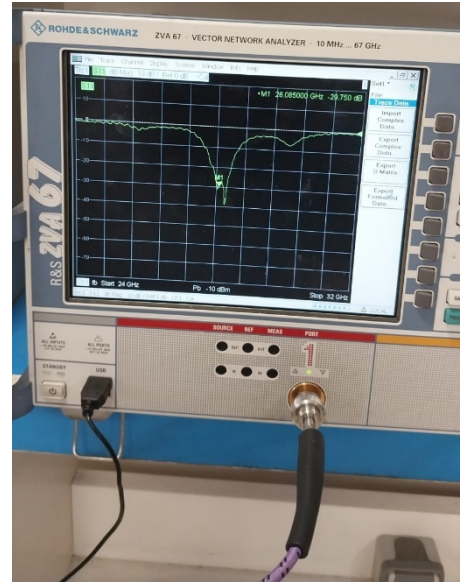


Figure 12. 2D radiation pattern



(a)



(b)

Figure 13. Fabricated antenna (a) The prototype (b) The measured.

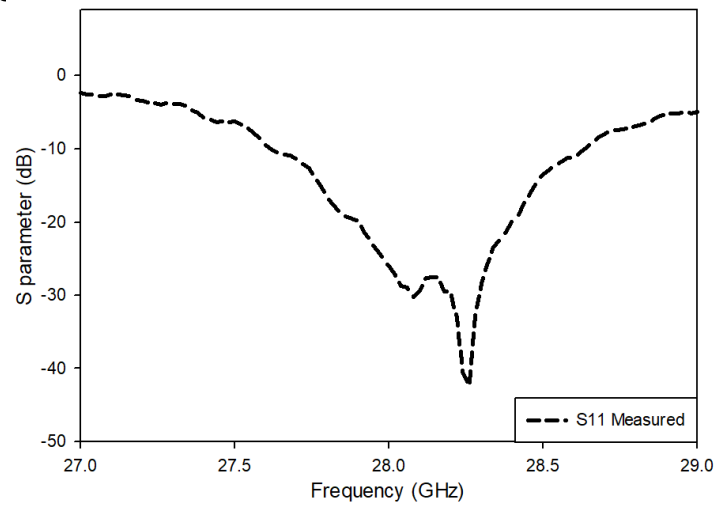


Figure 14. The Measured Reflection Coefficient of Array.

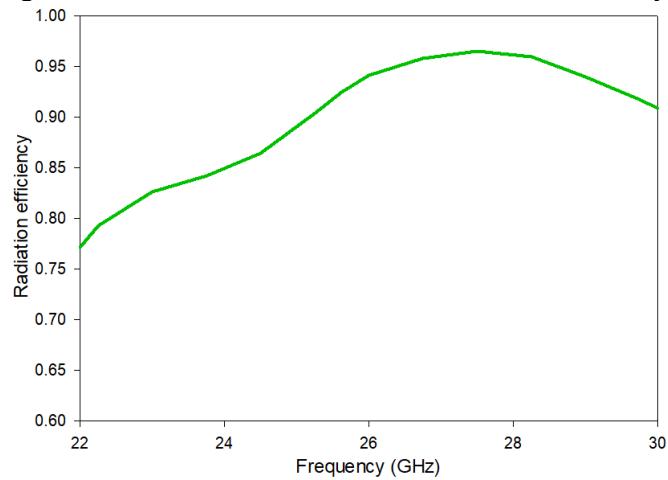


Figure 15. The Antenna Array Radiation Efficiency.

On the contrary, our proposed radiator shows lower efficiency and bandwidth compared to the suggested design, with more radiators than the suggested antenna, as indicated in Table 2.[29] Achieved superior gains compared to previous studies, as seen in Table 2. Our suggested radiator is more efficient compared to that of [39]– [44], which includes existing properties such as bandwidth, reflection coefficient, and VSWR.

Table 2: Comparison Between our Suggested Antenna and other Studies

Ref	No. of antenna	S11 (dB)	Gain (dB)	Dir. (dB)	BW. (GHz)	VSWR	Effic.	Size (mm)
[28]	-	-31	5.99	-	3.98	-	-	57.5 x 5
[39]	-	-22	9.8	-	1.5	-	84	18.6x18.6
[40]	-	-30	10	10.6	0.52	-	97	156x76
[41]	2 x 2	-85	13.5	14.1	1.14	1	93	100x60
[42]	1 x 2	-23	9.5	-	-	1.3	-	14.7x7.6
[43]	5	-30	11	-	1	-	-	26.5x18
[34]	13	-22	8.4	-	0.9	-	92	-
The work	4	-34	11	11.1	2.56	1.09	97	32.8 x 18

4. Conclusion

This article proposes a single-patch antenna with a compact design optimized for 28 GHz 5G frequency. Subsequently, we employ this component to implement a design that includes a 1 x 4 linear antenna array, each with many rectangular and circular slots for 28 GHz 5G operating frequency. The array is connected using a 1 x 4 junction power divider, ensuring equal amplitude and zero phase distribution. This article presents the following results: a compact antenna with a low profile and high gain value. The suggested radiator has a bandwidth value of 2.56 GHz, reflection coefficients S11 -34 dB, VSWR 1.09, efficiency of 97%, and gain of 11 dB. The results from this product are excellent, especially when comparing directivity, bandwidth, gain, VSWR, and radiation efficiency to other references. Positioning the radiator array as a viable option for current 5G base station applications.

REFERENCES

- [1] L. Wang, M. Q. Yuan, and Q. H. Liu, "A dual-band printed electrically small antenna covered by two capacitive split-ring resonators," *IEEE Antennas Wirel Propag Lett*, vol. 10, pp. 824–826, 2011.
- [2] E.-S. Abdelhafid *et al.*, "Very low phase noise voltage controlled oscillator for 5G mm-wave communication systems," in *2020 1st international conference on innovative research in applied science, engineering and technology (IRASET)*, IEEE, 2020, pp. 1–4.
- [3] Q. M. Gatea, N. Al-Kafahji, F. M. Ali, and A. J. Alyasiri, "Hash unit cell shape used to enhancement gain and bandwidth of metasurface antenna," in *Journal of Physics: Conference Series*, IOP Publishing, 2020, p. 12022.
- [4] Q. M. Gatea, F. M. Ali, N. Al-Kafahji, and A. J. Alyasiri, "Gradient distribution of metasurface based antenna performance enhancement," in *AIP Conference Proceedings*, AIP Publishing, 2020.
- [5] Z. Ding *et al.*, "Application of non-orthogonal multiple access in LTE and 5G networks," *IEEE Communications Magazine*, vol. 55, no. 2, pp. 185–191, 2017.
- [6] Q. M. Gatea, N. Al-Kafahji, F. M. Ali, and H. Al-Saedi, "Design dual-layer metasurfaces antenna for wireless application," in *AIP Conference Proceedings*, AIP Publishing, 2023.
- [7] A. Es-Saqy *et al.*, "28 GHz balanced pHEMT VCO with low phase noise and high output power performance for 5G mm-wave systems," *International Journal of Electrical and Computer Engineering*, vol. 10, no. 5, p. 4623, 2020.
- [8] M. Boumaiz, M. El Ghazi, S. Mazer, M. El Bekkali, A. Bouayad, and M. Fattah, "Performance analysis of DQPSK and DBPSK modulation schemes for a scheduled access phase based Wireless Body Area Network," in *2018 9th International Symposium on Signal, Image, Video and Communications (ISIVC)*, IEEE, 2018, pp. 163–167.
- [9] A. Maroua and F. Mohammed, "Characterization of ultra wide band indoor propagation," in *2019 7th Mediterranean congress of telecommunications (CMT)*, IEEE, 2019, pp. 1–4.

- [10] W. Hong *et al.*, "Multibeam antenna technologies for 5G wireless communications," *IEEE Trans Antennas Propag*, vol. 65, no. 12, pp. 6231–6249, 2017.
- [11] Q. M. Gatea, M. A. Alkhafaji, and M. T. Güneşer, "Design and simulation for triple-band metasurface slot antenna," in *AIP Conference Proceedings*, AIP Publishing, 2023.
- [12] M. J. Marcus, "5G and" IMT for 2020 and beyond"[Spectrum Policy and Regulatory Issues]," *IEEE Wirel Commun*, vol. 22, no. 4, pp. 2–3, 2015.
- [13] S. Sridevi and K. Mahendran, "Design of millimeter-wave microstrip patch antenna for MIMO communication," *International Research Journal of Engineering and Technology*, vol. 4, no. 10, pp. 1513–1518, 2017.
- [14] S. Didi, I. Halkhams, M. Fattah, Y. Balboul, S. Mazer, and M. El Bakkali, "Study and design of printed rectangular microstrip antenna arrays at an operating frequency of 27.5 GHz for 5G applications," 2021.
- [15] Q. M. Gatea, "Array of Slot Metasurface Units Cell for Wireless Application," in *2022 Iraqi International Conference on Communication and Information Technologies (IICCIT)*, IEEE, 2022, pp. 114–119.
- [16] A. A. R. Saad and H. A. Mohamed, "Printed millimeter-wave MIMO-based slot antenna arrays for 5G networks," *AEU-International Journal of Electronics and Communications*, vol. 99, pp. 59–69, 2019.
- [17] I.-J. Hwang, B. Ahn, S.-C. Chae, J.-W. Yu, and W.-W. Lee, "Quasi-Yagi antenna array with modified folded dipole driver for mmWave 5G cellular devices," *IEEE Antennas Wirel Propag Lett*, vol. 18, no. 5, pp. 971–975, 2019.
- [18] R. Thandaiah Prabu, M. Benisha, V. Thulasi Bai, and R. Ranjeetha, "Design of 5G mm-wave antenna using line feed and corporate feed techniques," in *Smart Intelligent Computing and Applications: Proceedings of the Second International Conference on SCI 2018, Volume 1*, Springer, 2019, pp. 367–380.
- [19] M. Roodaki-Lavasani-Fard, S. Sinha, C. Soens, G. A. E. Vandebosch, K. Mohammadpour-Aghdam, and R. Faraji-Dana, "Shared aperture dual-wideband planar antenna arrays using any-layer PCB technology for mm-wave applications," *IEEE Trans Antennas Propag*, vol. 70, no. 2, pp. 1087–1096, 2021.
- [20] M. M. M. Ali and A. Sebak, "Printed RGW circularly polarized differential feeding antenna array for 5G communications," *IEEE Trans Antennas Propag*, vol. 67, no. 5, pp. 3151–3160, 2019.
- [21] N. Ojaroudi Parchin *et al.*, "Frequency reconfigurable antenna array for mm-Wave 5G mobile handsets," in *Broadband Communications, Networks, and Systems: 9th International EAI Conference, Broadnets 2018, Faro, Portugal, September 19–20, 2018, Proceedings 9*, Springer, 2019, pp. 438–445.
- [22] L. G. Ayalew and F. M. Asmare, "Design and optimization of pi-slotted dual-band rectangular microstrip patch antenna using surface response methodology for 5G applications," *Heliyon*, vol. 8, no. 12, 2022.
- [23] W. A. Awan, M. Soruri, M. Alibakhshikenari, and E. Limiti, "On-Demand Frequency Switchable Antenna Array Operating at 24.8 and 28GHz for 5G High-Gain Sensors Applications.," *Progress In Electromagnetics Research M*, vol. 108, 2022.
- [24] H. Zahra, W. A. Awan, N. Hussain, S. M. Abbas, and S. Mukhopadhyay, "Helix inspired 28 GHz broadband antenna with end-fire radiation pattern," *Computers, Materials and Continua*, vol. 70, no. 1, pp. 1935–1944, 2022.
- [25] W. A. Awan, M. Alibakhshikenari, and E. Limiti, "High gain dual parasitic patch loaded wideband antenna for 28 GHz 5G applications," in *2021 International Symposium on Antennas and Propagation (ISAP)*, IEEE, 2021, pp. 1–2.
- [26] N. Hussain, W. A. Awan, W. Ali, S. I. Naqvi, A. Zaidi, and T. T. Le, "Compact wideband patch antenna and its MIMO configuration for 28 GHz applications," *AEU-International Journal of Electronics and Communications*, vol. 132, p. 153612, 2021.
- [27] H. Zahra, W. A. Awan, W. A. E. Ali, N. Hussain, S. M. Abbas, and S. Mukhopadhyay, "A 28 GHz broadband helical inspired end-fire antenna and its MIMO configuration for 5G pattern diversity applications," *Electronics (Basel)*, vol. 10, no. 4, p. 405, 2021.
- [28] S. Ashraf, J. A. Sheikh, and Z. A. Bhat, "A high gain multi slotted and compact planar microstrip millimeter wave antenna for 5G networks," *Progress In Electromagnetics Research M*, vol. 108, pp. 175–186, 2022.
- [29] S.-E. Didi, I. Halkhams, M. Fattah, Y. Balboul, S. Mazer, and M. El Bakkali, "Design of a microstrip antenna patch with a rectangular slot for 5G applications operating at 28 GHz," *TELKOMNIKA (Telecommunication Computing Electronics and Control)*, vol. 20, no. 3, pp. 527–536, 2022.

- [30] A. Es-Saqy *et al.*, “A 5G mm-wave compact voltage-controlled oscillator in 0.25 μm pHEMT technology,” *International Journal of Electrical and Computer Engineering*, vol. 11, no. 2, p. 1036, 2021.
- [31] S.-E. Didi, I. Halkhams, M. Fattah, Y. Balboul, S. Mazer, and M. El Bakkali, “Design of a microstrip antenna two-slot for fifth generation applications operating at 27.5 GHz,” in *International Conference on Digital Technologies and Applications*, Springer, 2021, pp. 1081–1089.
- [32] Q. M. Gatea and F. M. Ali, “Exploring Various Switching Techniques Employed in Designing a Reconfigurable Antenna: A Review,” in *International Conference On Innovative Computing And Communication*, Springer, 2024, pp. 647–666.
- [33] A. El Ansari, S. Das, I. Tabakh, B. T. P. Madhav, A. Bendali, and N. E. A. El Idrissi, “Design and Realization of a broadband multi-beam 1×2 array antenna based on 2×2 Butler Matrix for 2.45 GHz RFID Reader Applications,” *Journal of Circuits, Systems and Computers*, vol. 31, no. 17, p. 2250305, 2022.
- [34] A. El Ansari, T. Islam, S. V Rama Rao, A. Saravanan, S. Das, and N. E. A. El Idrissi, “A Broadband Microstrip 1×8 Magic-T Power Divider for ISM Band Array Antenna Applications,” 2023.
- [35] A. El Ansari, L. Kabouri, and E. Ahouzi, “Random attack on Asymmetric Cryptosystem based on phase-truncated fourier transforms,” in *2014 International Conference on Next Generation Networks and Services (NGNS)*, IEEE, 2014, pp. 65–68.
- [36] U. Ullah, M. Al-Hasan, S. Koziel, and I. Ben Mabrouk, “A series inclined slot-fed circularly polarized antenna for 5G 28 GHz applications,” *IEEE Antennas Wirel Propag Lett*, vol. 20, no. 3, pp. 351–355, 2021.
- [37] Q. M. Gatea, M. A. Alkhafaji, M. T. Guneser, and A. J. Obaid, “Wideband and High Gain Antenna of Flowers Patches for Wireless Application,” in *International Conference on Frontiers of Intelligent Computing: Theory and Applications*, Springer, 2023, pp. 433–445.
- [38] Y. Rahayu and M. I. Hidayat, “Design of 28/38 GHz dual-band triangular-shaped slot microstrip antenna array for 5G applications,” in *2018 2nd international conference on telematics and future generation networks (TAFGEN)*, IEEE, 2018, pp. 93–97.
- [39] M. Nabil and M. M. A. Faisal, “Design, simulation and analysis of a high gain small size array antenna for 5G wireless communication,” *Wirel Pers Commun*, vol. 116, no. 4, pp. 2761–2776, 2021.
- [40] H.-C. Huang, Y. Wang, and X. Jian, “Novel integrated design of a dual-band dual-polarization 5G mm-wave antenna array fed by FPCs with a U-slotted full-metal case for a cellular phone,” in *2019 International Workshop on Antenna Technology (iWAT)*, IEEE, 2019, pp. 50–53.
- [41] M. S. Sharawi and M. Ikram, “Slot-based connected antenna arrays for 5G mobile terminals,” in *2018 International Workshop on Antenna Technology (iWAT)*, IEEE, 2018, pp. 1–3.
- [42] D. Mungur and S. Duraikannan, “Design and analysis of 28 GHz millimeter wave antenna array for 5G communication systems,” *Journal of Science Technology Engineering and Management-Advanced Research & Innovation*, vol. 1, no. 3, p. 10, 2018.
- [43] J. Khan, D. A. Sehrai, and U. Ali, “Design of dual band 5G antenna array with SAR analysis for future mobile handsets,” *Journal of Electrical Engineering & Technology*, vol. 14, pp. 809–816, 2019.
- [44] C. K. Ali and M. H. Arif, “Dual-band millimeter-wave microstrip patch array antenna for 5G smartphones,” in *2019 International Conference on Advanced Science and Engineering (ICOASE)*, IEEE, 2019, pp. 181–185.